Use of Municipal Solid Waste Incinerator (MSWI) Fly Ash in Alkali Activated Slag Cement

Kang Huang, Xiaohui Fan, Min Gan and Zhiyun Ji

Abstract This paper investigates the utilization of municipal solid waste incinerator fly ash (MFA) as a replacement of alkali-activated slag (AAS) cement. The mechanical performance of pastes with different dosages of MFA were studied and optimized. Compared with the AAS no MFA added, the compressive strength of the AAS pastes prepared at 3 d(days) with a 10% replacement of MFA fell sharply from 71.11 to 48.25 MPa, which remained stable with more MFA added. When the replacement proportion increased to 30%, the AAS pastes still reached a high compressive strength of 64.37 MPa at 28 d. XRD and SEM analysis were conducted to investigate the hydration products and micro structure of pastes. Main hydration products of the AAS paste with 30% MFA addition were calcium silicate hydrate (C-S-H) gel and C-A-S-H (C-CaO; A-Al_2O_3; S-SiO_2; H-H_2O) gel. Some unreacted MFA particles could be also observed from SEM analysis. This study provides a new resource utilization way of MFA.

Keywords Ground granulated blast furnace slag · MSWI fly ash
Compressive strength · Hydration product

K. Huang (✉) · X. Fan · M. Gan · Z. Ji
School of Minerals Processing & Bioengineering, Central South University, No.932, South Lushan Road, Changsha 410083, Hunan, People's Republic of China
e-mail: 165612119@csu.edu.cn

X. Fan
e-mail: csufanxiaohui@126.com

M. Gan
e-mail: csuganmin@126.com

Z. Ji
e-mail: zhiyunji@sina.com

B. Li et al. (eds.), *Characterization of Minerals, Metals, and Materials 2019*, The Minerals, Metals & Materials Series,
https://doi.org/10.1007/978-3-030-05749-7_40

Introduction

Incineration is a commonly accepted solution throughout the world for managing the increasing production of Municipal Solid Waste (MSW). Although incineration reduces the volume of MSW and provides energy, it is not a final solution since it generates bottom and fly ashes that must subsequently be disposed of [1]. The fly ashes are collected from the flue gas by the air pollution control (APC) devices, consisting of fine particles that contain leachable heavy metals and highly toxic organic substances (dioxins and furans). It is therefore classified as a toxic waste that poses the more serious environmental problems. Many works have been done on the treatment of MSWI fly ash, such as cement-based solidification/stabilizations technology, thermo plasticity microencapsulation technology and glass technology [2]. Among them the most popular approach to minimize the environmental pollution of heavy metal contaminations is the cement-based technology due to the low cost and the fact that the main components of MSWI fly ash are similar to cement. The cement base materials solidification has been considered as the best technology to dispose the harmful wastes by the United States Environmental Protection Agency [3, 4]. However, the traditional cement industry consumes lots of energy and releases a large amount of greenhouse gas. Besides, the S and Cl in MSWI fly ash do great harm to the durability of cement products [5].

Ground granulated blast furnace slag (BFS) is one of the main by-products discharged from the steel industry. During the production of pig iron, 200–300 kg of BFS is generated per ton of pig iron. The output of BFS is more than 210 million tons in 2017 in China according to the World mineral production report by the British geological survey [6]. The negative impact on the environment caused by BFS and other metallurgical slags becomes more and more severe, thus how to utilize or reuse them is a significant issue [7]. But it has a latent hydraulic reactivity, which can be activated by proper activators such as lime, gypsum and alkali metal hydroxides, carbonates or silicates to form cementitious materials [8]. Alkali-activated materials offer a viable low-CO_2 alternative to Portland cement in numerous applications and exhibit desirable physical properties, as well as a potential reduction in CO_2 emissions by as much as 80% [9].

So, finding a greener and more eco-friendly way to utilize the poisonous MFA is imperative. It is reported that the alkali-activated slag cements have a great performance in mechanical properties, heavy metal solidification, corrosion resistance and durability. Meanwhile, the main component of MFA are CaO, SiO_2 and Al_2O_3, which is similar to the BFS. From the above, it is possible to use MFA as a replacement of alkali-activated slag cement to activate the potential cementitious property of MFA and solidify the heavy metal in MFA.

This work aimed to study the influences of MFA used as a replacement of alkali activated slag cement. The effect of the replacement levels of BFS by fly ash on compressive strength, scanning electron micrographs (SEM) and x-ray diffraction

Table 1 Chemical composition of BFS and MSWI fly ash

	CaO	SiO_2	MgO	Al_2O_3	S	K_2O	Na_2O	Cl
BFS	36.37	29.43	10.31	12.06	1.11	0.45	0.50	–
MFA	16.99	37.61	1.45	10.66	–	1.68	1.49	2.82

(XRD) of pastes were presented. This study would lay a groundwork for the future utilization of MSWI fly ash in the construction product and lead to reduce cement consumption and carbon dioxide emissions.

Experimental

Materials Characterization

BFS used in this study was supplied by a steel company in Hebei, China. MSWI fly ash obtained from a municipal solid waste incineration plant in Changde, Hunan Province. MSWI fly ash was divided into two bottom ash and fly ash, as well it could also be divided into grate furnace and fluidized fly ash. In this study fluidized fly ash was used. The chemical composition of BFS and MFA are shown in Table 1. The chemical constituents of the BFS include CaO (36.37 wt%), SiO_2 (29.43 wt%), Al_2O_3 (12.06 wt%) and MgO (10.31 wt%), while the main constituents of MFA are CaO (16.99 wt%), SiO_2 (37.61 wt%) and Al_2O_3 (10.66 wt%). Chemical grade NaOH and sodium silicate solution with the molar ratio of SiO_2 to Na_2O of 3.3 were used as reagents.

The particle size distribution of BFS and MFA are shown in Fig. 1. It is clearly known that BFS has a finer grain size than MFA, since most of BFS particle size was distributing below 20 μm when most of MFA particle size was distributing at 10–100 μm. Thus, BFS used in our study has great cementitious property due to its extremely fine grain size.

The XRD patterns of the raw material of MFA and BFS (Fig. 2) was obtained, and the results are shown in Fig. 2. The main mineral components of MFA were quartz, tobermorite and gismondine which contained a large amount of crystalline structure, causing low cementitious property of MFA. Figure 2b shows the XRD pattern of the BFS, indicating that the BFS is amorphous and the main phases are calcium silicon ($CaSi_2O_5$, CaSi) and merwinite ($Ca_3Mg(SiO_4)_2$).

Specimen Preparation and Testing

The alkaline activator solution was prepared by mixing sodium silicate solution and sodium hydroxide with modulus of 1.5. The MFA content were varied at 10, 20, 30, 40 and 60% to develop cement pastes. The water/binder ratio was calculated so

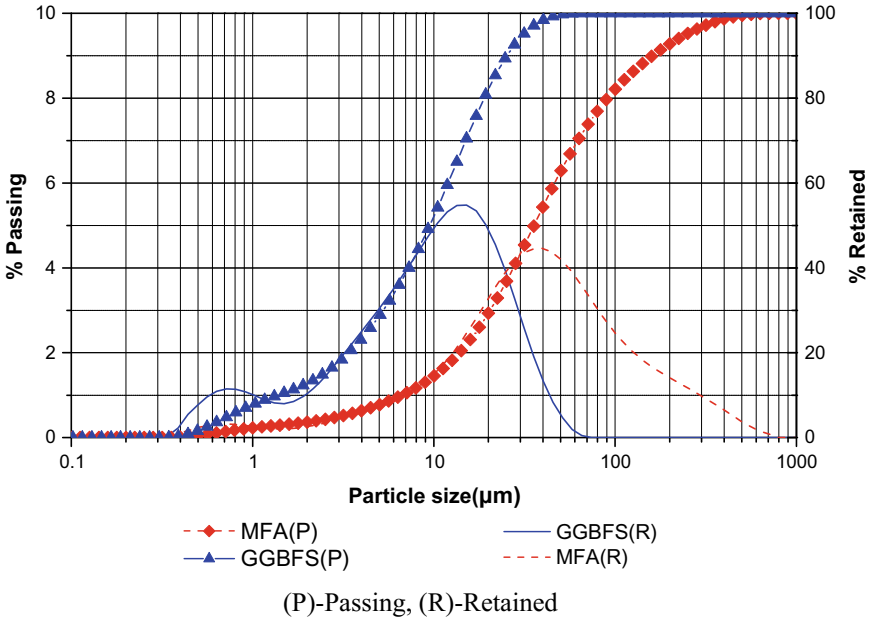

Fig. 1 Particle size distribution of MFA and BFS

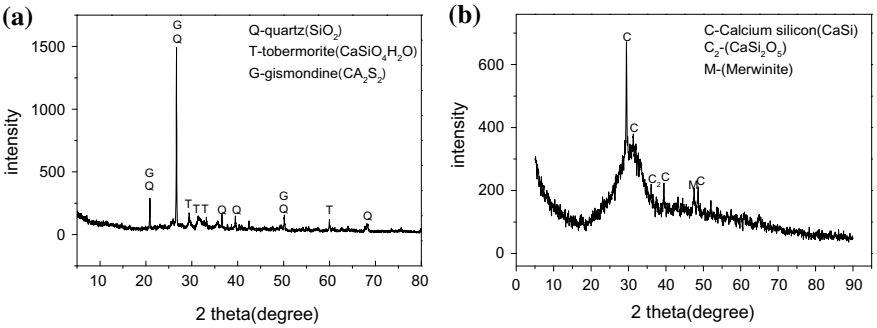

Fig. 2 XRD pattern of MFA (**a**), and BFS (**b**)

that the water stands for the total amount of water in the system (the water from the activator solution + the water added for the proper consistency) and binder represents the sum of the BFS and MFA mass and the solid part of the activator solution. Then the water/binder ratio was investigated at 0.4–0.6. The content of this activator solution was evaluated by the mass proportion of Na_2O to BFS and MFA. Additionally, the content of this activator solution was also changed from 5 to 10%. For all pastes, the modulus of alkaline activator solution was 1.5.

The mixing was done in an air-conditioned room at approximately 23 °C. Directly after mixing, the fresh paste was poured in the 20 mm × 20 mm × 20 mm cubic

moulds. The samples and moulds were covered with a vinyl sheet to prevent moisture loss and the carbonation of the surface. One batch of these samples were placed in an air-conditioned room at 23 °C for 3, 7, and 28 d.

The compressive strength results of pastes were measured on the cubic samples of dimension 20 mm × 20 mm × 20 mm. Also, the microstructural characteristics of paste, which was made at the optimum condition and had a high compressive strength, was analyzed using X-ray diffraction (XRD) and scanning electron microscope-energy dispersive spectroscopy (SEM-EDS).

Results and Discussion

Compressive Strength

Compressive strength of pastes with varying MFA/(BFS + MFA) ratio is given in Fig. 3. The content of MFA in the paste was supposed to be the most important parameter for the compressive strength. Paste without MFA addition had an extremely high early compressive strength of 71.11 MPa at 3d. A significant decrease of compressive strength happened with the addition of MFA. However, the compressive strength stayed stable with slow decrease relatively when more MFA added to this system. It could be concluded that the MFA appeared a low cementitious property and most of MFA particles were applied to be fine aggregate in this system. The decline of compressive strength at 7d increased when the ratio of MFA/(BFS + MFA) changed from 0.3 to 0.4. Thus, the proper ratio of MFA/(BFS + MFA) chosen in this work is 0.3 and following pastes were prepared at this ratio.

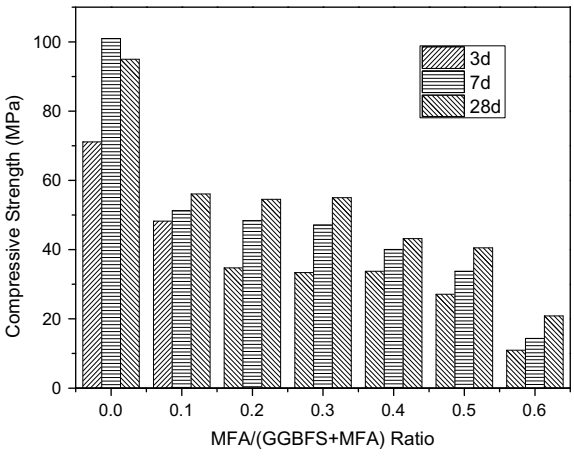

Fig. 3 Compressive strength of pastes with varying MFA/(BFS + MFA) ratio

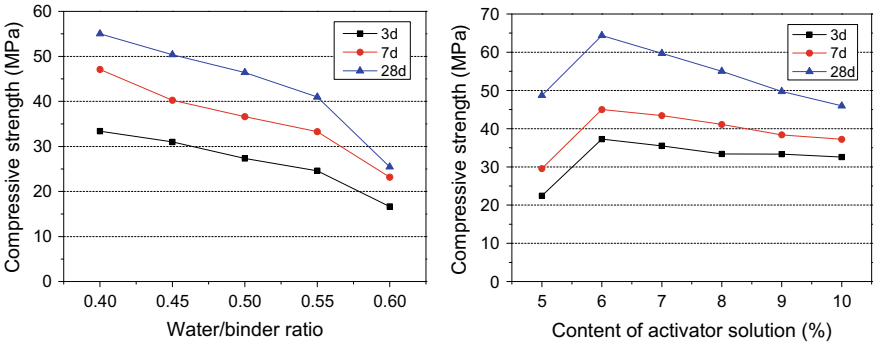

Fig. 4 Compressive strength of pastes with different water/binder ratio and content of activator solution to BFS + MFA

Figure 4 plots the compressive strength of pastes with different water/binder ratio. In order to keep the mobility of the slurry, the minimum of water/binder ratio was 0.4. The water/binder ratio determines the initial porosity of the cementitious system. The initial porosity would be greater at bigger water/binder ratio. At the same time, low water/binder ratio provides high alkaline concentration that the materials could be activated better. Thus, increasing of water/binder ratio resulted in decrease of compressive strength of these pastes. Highest compressive strength was obtained when water/binder ratio was 0.4.

The influence of activator solution content (5–10%) on compressive strength can also be seen in Fig. 4. The content of the activator solution also plays an important role in determining compressive strength of pastes. The compressive strength of the paste at the activator solution content of 5% was relatively poor. This is because the low activator solution content could not provide a fully high concentration of alkaline in the system, thus the materials were unable to be activated completely. Higher compressive strength was obtained with ratio of Na_2O/(BFS + MFA) at 6–8%, and at this range the increase of compressive strength was not evident with the increase of activator solution content. It indicated that the material could be activated well at the content of alkaline activator at 6%. So, considered about the cost of alkaline activator, less activator solution content of 6% would be adapted to this system.

Therefore, at the mass content of MFA was 30%, the best water/binder ratio and activator solution content was 4% and 6%. When these pastes were cured at 23 °C for 3, 7 and 28d, the compressive strength values were 37.28, 45.00, and 64.27 MPa, respectively. And the paste under optimal conditions (P-30MFA) was chosen to investigate microstructural and hydration products.

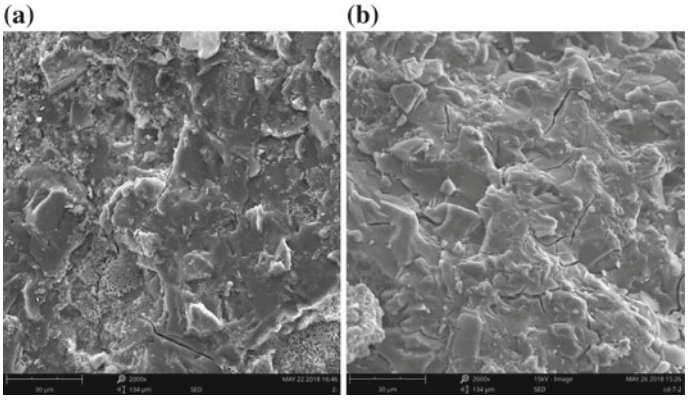

Fig. 5 SEM micrographs of P-30MFA at 3d (**a**), and 7d (**b**)

Table 2 Atom percentages and ratios of position A and B as shown in Fig. 6

Position	O	Na	Al	Si	Ca	Mg
A	73.52	6.92	3.83	8.93	5.14	1.66
B	65.26	7.20	3.73	13.23	9.03	1.54

Microstructural Analysis

Figure 5 shows micrographs of the surface of paste (P-30MFA) under optimal conditions at different ages of 3d and 7d respectively. It is commonly acknowledged that calcium silicate hydrate (C-S-H) is the major binding phase in AAS pastes. It is clearly observed that compact C-S-H gel was formed and some C-S-H gel in hydration after curing age of 3d in Fig. 5a. The morphologies became more compact with increase of curing age and the hydration reaction almost finished at 7d in Fig. 5b, indicated that the paste was becoming more and more dense with the increase of curing age with the pozzolanic reaction proceeding. SEM observations prove that the microstructure of the samples is very compact which may be explained by the formation of amorphous C-S-H phase, being the major binding phase of the pastes.

Figure 6 shows a representative scanning electron micrograph of P containing 70 wt% of BFS and 30 wt% of MFA at 7 days. This micrograph was representative of the microstructural features found in such systems at this stage of the hydration process. EDS analysis was conducted on the paste and the results are summarised in Table 2.

As is shown in the picture, element composition was different obviously in these two position. Two particles were found in this picture had same micro morphology as the unreacted MFA particles, and the element composition of position A was similar

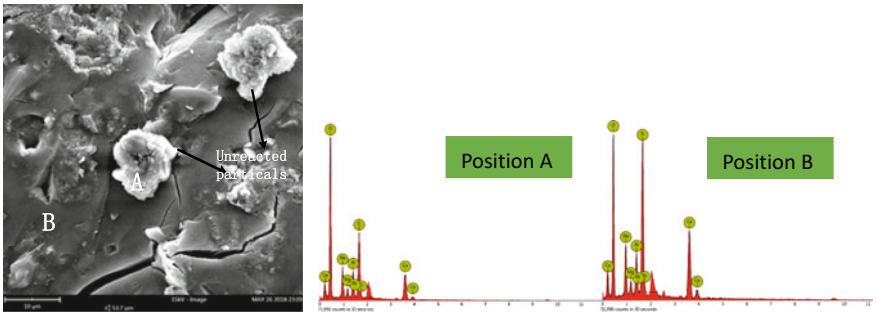

Fig. 6 SEM and EDS results of P-30MFA at 7 days

to the MFA. So this two particles were identified as unreacted MFA particles. It was found that the elemental composition of position B was dominated by silicon and calcium. The main reaction product generally cited for alkali-activated slag is C-S-H gel similar to that found in PC but with lower Ca/Si ratios (around 0.7) [10]. In position B, it could be calculated that the Ca/Si ratio is 0.68 as is shown in the Table 2. Thus, position B was suggested to be C-S-H gel binder with Ca/Si ratio of nearly 0.7 and this result showed that the addition of MFA had a inconspicuous impact on the hydration reaction. It is notable that the Al coexist in the position B, with a Al/Si = 0.28, and this could be deem to the Al in the system replaces the silicon in bridging positions. Fernández-Jiménez et al. and Brough and Atkinson [10, 11] reported that the use of waterglass as an alkali activator induces the formation of a C-A-S-H gel with high Si Q^2 and Q^3 or Q^{Poly} contents and the formation of long, intertwined chains. Therefore in this system, the fomation of C-A-S-H gel was also could be inferred by SEM-EDS analysis.

XRD Analysis

The XRD patterns of the P-30MFA (Fig. 7) at 3d, 7d and 28d were obtained. The main component of P-30MFA were calcite, C-S-H gel and quartz. The peak of quartz was due to the high SiO_2 oxide compositions in MFA. Calcite could also be observed in this system resulting from carbonation. In a non-crystalline state, diffraction of X-rays resulted in a broad diffuse halo rather than sharp diffraction peaks. The broad and amorphous hump from 20° to 40° (2θ) was the characteristic peak of amorphous gel including calcium silicate hydrate (C-S-H) gel and calcium aluminosilicate hydrate (C-A-S-H) gel.

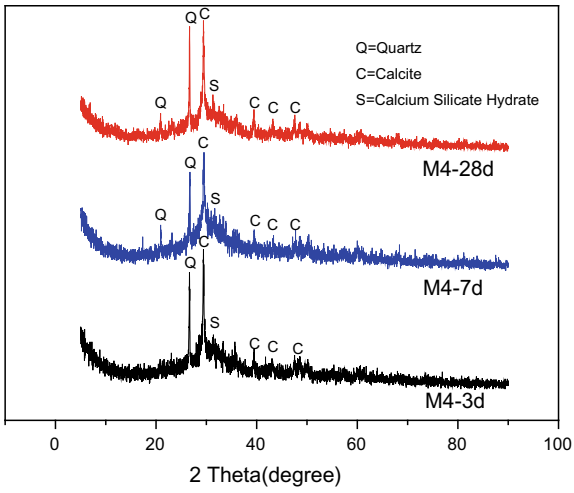

Fig. 7 X-ray diffraction (XRD) of P-30MFA at 3d, 7d and 28d

Conclusions

In this paper, compressive strength and micro structural characteristics of AAS paste with MFA addition were studied. The following conclusions can be drawn.

1. The use of MFA in alkali activated slag cement resulted in a sharp decrease of compressive strength and it could be concluded that the most MFA particles were crystalline structure. A relatively high compressive strength was obtained at a mass ratio of MFA/(BFS + MFA) is 0.3, activated by the activator solution, with the modulus of 1.5 and water/binder ratio of 0.4 and the proper content of this mixed activator was 6%. The compressive strength of these pastes was 64.37 MPa when they were cured at 23°C for 28d.
2. With the increase of curing age, the morphologies became more compact and the hydration reaction almost finished. C-S-H gel and C-A-S-H gel could be found in this phase with unreacted MFA particles.
3. The XRD patterns showed the main components of P-30MFA were calcite, C-S-H gel and quartz. The peak of quartz was due to the high SiO_2 oxide compositions in MFA, indicate that some MFA particles were not being activated due to its crystalline structure. Calcite could also be observed in this system resulting from carbonation. The broad and amorphous hump from 20° to 40° (2θ) was the characteristic peak of amorphous gel including C-S-H gel and C-A-S-H gel.

Acknowledgements The research was financially supported by the National Natural Science Foundation of China (No. U1660206, U1760107), Hunan Provincial Co-Innovation Center for Clean and Efficient Utilization of Strategic Metal Mineral Resources and Innovation Driven Plan of Central South University (No. 2015CX005) and Hunan Key Research & Development Plan (2018SK2049).

References

1. Ferreira C, Ribeiro A, Ottosen L (2003) Possible applications for municipal solid waste fly ash. J Hazard Mater 96(2–3): 201–216
2. Guo X, Shi H (2013) Self-solidification/stabilization of heavy metal wastes of class c fly ash-based geopolymers. J Mater Civ Eng 25(4):491–496
3. Jin M, Zheng Z, Sun Y et al (2016) Resistance of metakaolin-MSWI fly ash based geopolymer to acid and alkaline environments. J Non Cryst Solids 450:116–122
4. Minocha AK, Jain N, Verma CL (2003) Effect of inorganic materials on the solidification of heavy metal sludge. Cem Concr Res 33(10):1695–1701
5. Lederer J, Trinkel V, Fellner J (2016) Wide-scale utilization of MSWI fly ashes in cement production and its impact on average heavy metal contents in cements: the case of Austria. Waste Manag 60:247–258
6. Brown TJ, Idoine NE, Raycraft ER, Shaw RA, Deady EA, Hobbs SF, Bide T (2017) World mineral production 2011-2015. British Geological Survey, Nottingham
7. Shen JG, Guo CY, Chen M, Yu JK, Jian MF (2006) Utilization of metallurgical slag as resource materials in China. Dev Chem Eng Miner Process 14:487–493
8. Lecomte I, Henrist C, Liégeois M et al (2006) (Micro)-structural comparison between geopolymers, alkali-activated slag cement and Portland cement. J Eur Ceram Soc 26(16):3789–3797
9. Juenger MCG, Winnefeld F, Provis JL, Ideker JH (2011) Advances in alternative cementitious sbinders. Cem Concr Res 41:1232–1243
10. Fernández-Jiménez A, Puertas F, Sobrados I, Sanz J (2003) Structure of calcium silicate hydrates formed in alkaline activated slag. Influence of the type of alkaline activator. J Am Ceram Soc 86(3):1389–1394
11. Brough AR, Atkinson A (2002) Sodium silicate-based, alkali-activated slag mortars. Part I. Strength, hydration and microstructure. Cem Concr Res 32:865–879